Journal of Biomolecular NMR, 7 (1996) 89–98
ESCOM

J-Bio NMR 339

Chemical shift assignments and secondary structure of the Grb2 SH2 domain by heteronuclear NMR spectroscopy

Yu-Sen Wang*, Anne F. Frederick, Mary M. Senior*, Barbara A. Lyons**, Stuart Black, Paul Kirschmeier, Louise M. Perkins and Oswald Wilson

Schering-Plough Research Institute, 2015 Galloping Hill Road, Kenilworth, NJ 07033, U.S.A.

Received 21 November 1995
Accepted 6 February 1996

Keywords: Grb2; SH2 domain; Heteronuclear NMR; CSI method; Chemical shift assignments; Secondary structure; Isotopic enrichment

Summary

The growth factor receptor-bound protein-2 (Grb2) is an adaptor protein that mediates signal transduction pathways. Chemical shift assignments were obtained for the SH2 domain of Grb2 by heteronuclear NMR spectroscopy, employing the uniformly ^{13}C-/^{15}N-enriched protein as well as the protein containing selectively ^{15}N-enriched amino acids. Using the Chemical Shift Index (CSI) method, the chemical shift indices of four nuclei, $^{1}H^{\alpha}$, $^{13}C^{\alpha}$, $^{13}C^{\beta}$ and ^{13}CO, were used to derive the secondary structure of the protein. Nuclear Overhauser enhancements (NOEs) were then employed to confirm the secondary structure. The CSI results were compared to the secondary structural elements predicted for the Grb2 SH2 domain from a sequence alignment [Lee et al. (1994) *Structure*, **2**, 423–438]. The core structure of the SH2 domain contains an antiparallel β-sheet and two α-helices. In general, the secondary structural elements determined from the CSI method agree well with those predicted from the sequence alignment.

Introduction

Grb2 is an adaptor protein that mediates signal transduction pathways. It is the human homologue, both structurally and functionally, of Sem-5 from *Caenorhabditis elegans* (Clark et al., 1992) and of Drk from *Drosophila melanogaster* (Olivier et al., 1993). It is a 25-kDa protein consisting of one Src homology region-2 (SH2) domain and two Src homology region-3 (SH3) domains, arranged in the order SH3-SH2-SH3. The SH2 domain of Grb2 binds to specific tyrosine phosphorylation sites on several different proteins, including the oncogene product Shc and the EGF receptor (Downward, 1994; Pawson, 1995). The Grb2 SH2 domain recognizes the specific phosphotyrosine (pY) consensus sequence pYXNX, where X represents any amino acid and N represents asparagine (Songyang et al., 1994). The two SH3 domains of Grb2 bind to proline-rich sequences in the carboxyl region of the Son of sevenless (mSOS) protein. The formation of this phosphoprotein–Grb2–mSOS complex brings a significant portion of mSOS to the plasma membrane where its substrate, the $p21^{ras}$ protein, is located. The mSOS protein then activates $p21^{ras}$ through its guanine nucleotide exchange activity (Chardin et al., 1993). Thus, Grb2 plays a critical role in the activation of $p21^{ras}$, either directly, by binding to the EGF receptor, or indirectly, by binding to Shc.

As a class, SH2 domains are small, consisting of approximately 100 amino acid residues, and they are highly conserved among cytoplasmic signaling proteins. SH2 domains have been identified in both catalytic proteins (e.g. PLC-γ and GAP) and noncatalytic proteins (e.g. the p85α subunit of PI3K, Grb2, and crk). Despite the functional differences of SH2 domain-containing proteins, the structures of the SH2 domains appear to be homologous. A number of SH2 domain structures, with and without bound phosphopeptides, have been determined by both NMR spectroscopy (Booker et al., 1992; Overduin et al.,

*To whom correspondence should be addressed.
**Present address: Department of Biochemistry, College of Medicine, University of Vermont, Burlington, VT 05405, U.S.A.

Abbreviations: crk, viral $p47^{gag\text{-}crk}$; EGF, epidermal growth factor; GAP, GTPase-activating protein; PI3K, phosphatidylinositol-3-kinase; PLC-γ, phospholipase-C-γ; shc, src homologous and collagen; src, sarcoma family of nonreceptor tyrosine kinase.

0925-2738/$ 6.00 + 1.00 © 1996 ESCOM Science Publishers B.V.

1992a,b; Hensmann et al., 1994; Pascal et al., 1994; Narula et al., 1995; Xu et al., 1995; Zhou et al., 1995) and X-ray crystallography (Waksman et al., 1992,1993; Eck et al., 1993; Lee et al., 1994; Hatada et al., 1995). In this paper, we report the chemical shift assignments and secondary structure of the isolated SH2 domain of Grb2 as determined by heteronuclear NMR spectroscopy and the Chemical Shift Index (CSI) method (Wishart and Sykes, 1994).

Materials and Methods

Protein biosynthesis, purification, and NMR sample preparation

The SH2 domain is defined as residues 60–158 of the full-length Grb2 protein (Lowenstein et al., 1992). The recombinant protein used for the NMR studies presented here comprises residues 53–163 plus an N-terminal glycine, which is contributed by the expression plasmid. N-terminal amino acid sequencing indicates that the initiator methionine is post-translationally removed from the purified recombinant protein (data not shown). Thus, the purified protein contains eight additional residues N-terminal and five additional residues C-terminal to the consensus sequence of the SH2 domain. The residues N- and C-terminal to the SH2 domain are either residues connecting the SH2 domain to the two SH3 domains or residues that comprise the SH3 domains of Grb2. In this NMR study, we have chosen to number the protein starting with the N-terminal glycine as residue 1. Thus, as denoted in Fig. 1, the SH2 domain begins with Trp^{9} and ends with Pro^{107}.

DNA encoding the recombinant protein was subcloned into the pQE-60 plasmid and transformed into *E. coli* SG13009 cells (Qiagen, Chatsworth, CA). Uniform ^{15}N enrichment (Muchmore et al., 1989) and $^{13}C/^{15}N$ enrichment (McIntosh and Dahlquist, 1990) were achieved by growing the cells for 5 h at 37 °C in M9 minimal medium containing 1 g/l of $(^{15}NH_4)_2SO_4$ (Isotec, Inc., Miamisburg, OH) or 1 g/l of $(^{15}NH_4)_2SO_4$ and 3 g/l of ^{13}C-glucose (Cambridge Isotopes, Andover, MA), respectively. To label specific amino acid residues, *E. coli* strain DL39 was used (LeMaster and Richards, 1988). This particular strain is auxotrophic for leucine, valine, phenylalanine, isoleucine, tyrosine, and aspartic acid residues. Two protein samples, one with only leucine residues ^{15}N enriched and one with both valine and phenylalanine residues ^{15}N enriched, were produced by growing cells at 37 °C in fermentor medium, as previously described elsewhere (DeLoskey et al., 1994) with 230 mg/l of L-[^{15}N]leucine and with 230 mg/l of L-[^{15}N]valine and 130 mg/l of L-[^{15}N]phenylalanine (Cambridge Isotopes), respectively.

E. coli were induced with 1 mM IPTG at 30 °C for 2–3 h and then harvested. The overexpressed protein was purified by use of phosphotyrosine (Eck et al., 1993) and anion exchange chromatography. Protein yields for the cells grown in M9 minimal media for the ^{15}N and $^{13}C/^{15}N$ preparations were 9–10 mg/l. For the specifically labeled amino acid preparations, protein yields were 20 mg/l. The protein samples were judged to be greater than 95% pure by SDS-PAGE. N-terminal amino acid sequencing and amino acid analysis were employed to confirm the identity of the purified SH2 domain. The degree of both ^{15}N and ^{13}C enrichment was determined by mass spectrometry to be greater than 95%.

All protein samples were dialyzed against 5 mM sodium acetate, pH 5.0, containing 0.015% sodium azide. Using Centricon-10 micro-concentrators (Amicon, Beverly, MA), dialyzed samples were concentrated to a final NMR sample volume of 0.6 ml, yielding protein concentrations between 1.0 and 1.5 mM. The final pH of the concentrated protein samples was 5.3. Dynamic light scattering analysis (Protein Solutions, Inc., Charlottesville, VA) showed that under these solution conditions the protein was in the monomeric form for greater than 99% (data not shown).

NMR spectroscopy

NMR experiments collected on the uniformly ^{15}N- and ^{13}C-/^{15}N-enriched samples were performed on a Varian Unity-600^{+} spectrometer, equipped with pulsed field gradient units and a triple resonance probe with actively shielded Z gradients. NMR experiments carried out on the two selectively ^{15}N-enriched protein samples were acquired on an Omega GN500-PSG spectrometer, equipped with a triple resonance probe (Nalorac, Martinez, CA). The sample temperature for all NMR experiments was maintained at 25 °C.

Unity-600^{+} experiments Quadrature detection on the Unity-600^{+} spectrometer in the indirect dimensions was attained using the TPPI method (Marion and Wüthrich, 1983) or the States-TPPI method (Marion et al., 1989a). Water suppression was achieved either with a low-power presaturation pulse during the recycling delay or with pulsed field gradient selection (Kay et al., 1993). ^{15}N or ^{13}C decoupling during acquisition was accomplished using a GARP1 programmable pulse modulation sequence (Shaka et al., 1985). Where applicable, isotropic mixing was achieved with the DIPSI-3 mixing scheme (Shaka et al., 1988).

A two-dimensional (2D) ^{1}H-^{15}N HSQC correlation experiment (Bodenhausen and Ruben, 1980), a 3D ^{1}H-^{15}N HMQC-TOCSY experiment (Marion et al., 1989b), and a 3D ^{1}H-^{15}N NOESY-HMQC experiment (Marion et al., 1989b) were acquired on the uniformly ^{15}N-enriched protein sample in 90% H_2O/10% D_2O (Cambridge Isotopes). In all three ^{15}N-edited experiments, the proton transmitter (D1) was centered over the amide region at 7.5 ppm and in the ^{15}N dimension (D3) at 118.5 ppm. In the 3D experiments, the data were collected as a series of 2D ^{1}H-^{1}H

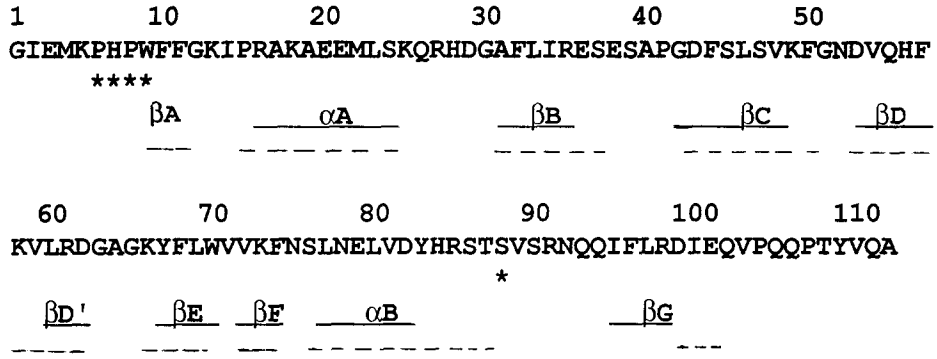

Fig. 1. Sequence of the protein analyzed by NMR spectroscopy. The consensus sequence of the SH2 domain begins at Trp^{9} and ends at Pro^{107}. The asterisks denote unassigned amino acid residues. Secondary structural elements obtained from the CSI method are designated with a solid line, while those obtained from the sequence alignment (Lee et al., 1994) are designated with a dashed line. The α-helices and β-strands are labeled according to the SH2 nomenclature previously established (Eck et al., 1993).

planes, which were edited by ^{15}N. The HMQC-TOCSY experiment was acquired with a 33 ms mixing time and a field strength of 11.7 KHz, and the NOESY-HMQC with mixing times of 50 and 125 ms. The 3D HCCH-TOCSY experiment (Bax et al., 1990) was acquired with gradient enhancement (Kay et al., 1993). The transmitters were centered at 3.00 ppm for ^{1}H and at 43.0 ppm for ^{13}C. The data were acquired as a series of 2D ^{1}H-^{1}H planes edited by ^{13}C, with a 17 ms mixing time and a field strength of 6.25 KHz. The spectral and data point parameters for these experiments are listed in Table 1.

Hydrogen/deuterium exchange experiments were carried out by lyophilizing the uniformly ^{15}N-enriched protein sample from 5 mM sodium acetate buffer, pH 5.3, and then redissolving the protein in 0.6 ml of D_2O. Eight 2D ^{1}H-^{15}N HSQC spectra were collected over a 24 h period, with the first spectrum collected 19.5 min after the D_2O addition. The 2D data sets were acquired as described above, except that the proton spectral width was 5000 Hz and 128 FIDs were collected with 16 scans per increment.

The triple resonance experiments, HNCA (Kay et al., 1990; Farmer et al., 1992), HN(CO)CA (Bax and Ikura, 1991), HNCO (Kay et al., 1990; Muhandiram and Kay, 1994), HNCACB (Wittekind and Mueller, 1993; Muhandiram and Kay, 1994), and CBCA(CO)NH (Grzesiek and Bax, 1992), were acquired on the ^{13}C-/^{15}N-enriched protein sample in 90% H_2O/10% D_2O. All triple resonance experiments were acquired with gradient selection, except for the HNCA experiment. In these experiments, the transmitters were centered as follows: ^{1}H (D1) over the amide region (7.5 ppm) or on residual HDO (4.8 ppm); ^{13}C (D2) in the center of the carbonyl region (175 ppm) or over the $^{13}C^{\alpha}$ region (43 ppm); and ^{15}N (D3) at 118.5 ppm. The HN(CO)CA, HNCO, and HNCACB pulse programs were implemented with constant time in the ^{15}N dimension and in both the ^{13}C and ^{15}N dimensions for the CBCA(CO)NH experiment. The spectral and data point parameters for these experiments are listed in Table 1.

Omega GN500-PSG experiments For the GN500 experiments, quadrature detection was achieved via the method of States et al. (1982), ^{15}N decoupling during acquisition with programmable WALTZ decoupling (Shaka et al., 1983), and isotropic mixing in the TOCSY-HMQC experiments with the clean MLEV-17 sequence (Griesinger et al., 1988). In all GN500 NMR experiments, residual water was suppressed with a low-power pre-

TABLE 1
VARIAN UNITY-600^{+} ACQUISITION PARAMETERS FOR NMR EXPERIMENTS ON UNIFORMLY ENRICHED SAMPLES

Experiment	Spectral widths (kHz)			Data points			Scans/point
	D1[a]	D2[b]	D3[c]	D1[a]	D2[b]	D3[c]	
2D HSQC	6.0	–	2.3	2048	–	1024	32
3D HMQC-TOCSY[d]	9.0	2.3	9.0	512	256	64	16
3D HCCH-TOCSY	5.0	5.0	3.1	512	128	32	16
3D NOESY-HMQC	6.0	9.0	2.3	512	128	22	16
HNCA	6.0	6.2	2.3	512	64	20	32
HNCOCA	8.0	6.3	2.3	512	64	32	32
HNCO	9.0	3.0	2.3	512	128	32	8
HNCACB	6.0	9.0	2.3	512	58	20	32
CBCA(CO)NH	9.0	9.0	2.3	512	60	32	32

[a] D1 refers to ^{1}H.
[b] D2 refers to ^{1}H or ^{13}C.
[c] D3 refers to ^{15}N.
[d] For this experiment, D1, D2 and D3 refer to ^{1}H, ^{15}N and ^{1}H, respectively.

saturation pulse. Protein resonances affected by the presaturation pulse were recovered using the SCUBA method (Brown et al., 1988).

2D ^{1}H-^{15}N HSQC correlation experiments were acquired for both the selectively ^{15}N-leucine- and ^{15}N-phenylalanine/^{15}N-valine-enriched samples. Each experiment was acquired with 2048 complex points and 512 FIDs, with 256 scans per point. Similar 2D experiments were collected for each sample using the TOCSY-HMQC and NOESY-HMQC experiments. In the TOCSY-HMQC experiments, mixing times of 45 and 65 ms were used. The mixing times used in the NOESY-HMQC experiments were 100 and 125 ms.

Proton chemical shifts were referenced externally to sodium 3-(trimethylsilyl)-propionate-2,2,3,3-d_4 (TSP) in 5 mM acetate buffer, pH 5.3, at 25 °C (0.00 ppm). ^{13}C chemical shifts were referenced externally to 10% aqueous dioxane at 25 °C (69.46 ppm) (Wishart and Sykes, 1994). ^{15}N chemical shifts were referenced externally to 2.9 M [^{15}N]-ammonium chloride in 1 M HCl at 37 °C (24.93 ppm) relative to liquid ammonia (Levy and Lichter, 1979).

Digitized NMR data were exported to an INDIGO-2 workstation (Silicon Graphics, Inc., Mountain View, CA), and then processed using FELIX v. 2.30 (Biosym Technologies, San Diego, CA). Both 2D and 3D data sets were processed using real matrices, with 3D matrices having dimensions of 512 (D1)×128 (D2)×64 (D3). Time domains in D1 were multiplied by 60° sine-bell functions prior to Fourier transformation. In the D2 and D3 dimensions, linear prediction routines were utilized before applying a squared sine-bell function, followed by zero-filling and Fourier transformation.

Results and Discussion

Resonance assignments

In the 2D ^{1}H-^{15}N HSQC spectrum, which correlates the ^{15}N and its attached H^N resonance, 106 non-proline residues were expected. The 89 residues that were actually observed are shown in Fig. 2. A total of 12 additional residues, Gly^{1}, Phe^{10}, Leu^{69}, Val^{81}, His^{84}, Val^{89}, Arg^{98}, Ile^{100}, and four residues at the C-terminus (Thr^{108} through Gln^{111}) were not observed in the HSQC spectrum, but

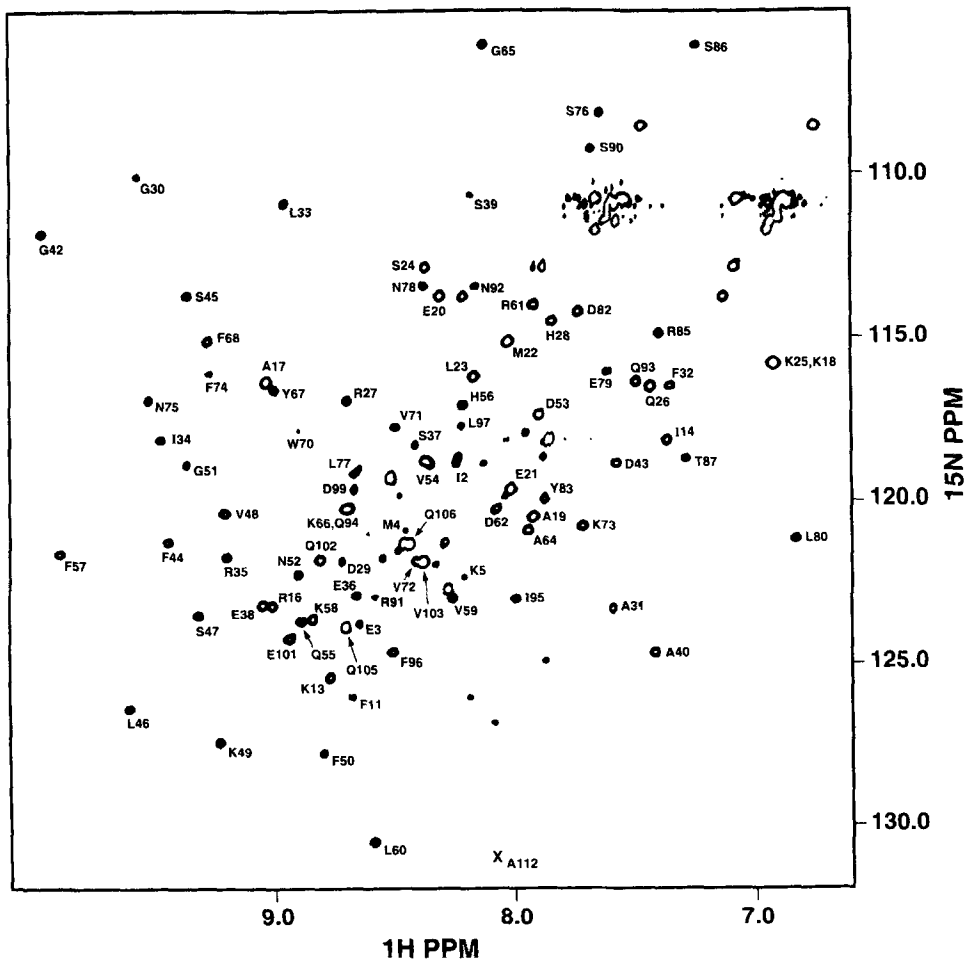

Fig. 2. An expanded contour plot from the 2D ^{1}H-^{15}N HSQC correlation experiment, depicting the assigned ^{15}N to H^N correlations in the Grb2 SH2 domain. Gly^{12} and Gly^{63} resonances are off scale. The X denotes Ala^{112}, which is not observable at this contour level.

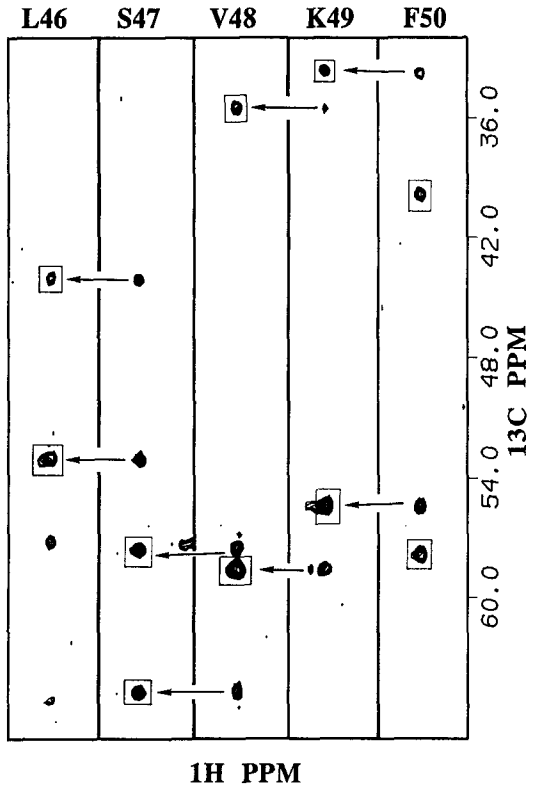

Fig. 3. Strip plots of amide resonances from several planes of the 3D triple resonance HNCACB spectrum, illustrating the use of $^{13}C^{\alpha}$ and $^{13}C^{\beta}$ resonances in the sequential assignment procedure. The amide resonances for these residues can be found in Table 2. Slices are taken at the ^{15}N frequency corresponding to the residue indicated at the top of each slice. Connectivities for Leu[46] through Phe[50] are shown. The intraresidue NH-$^{13}C^{\alpha}$ and NH-$^{13}C^{\beta}$ correlations are designated with boxes. Arrows connect the interresidue to the intraresidue correlations.

were detected and correlated to neighboring residues from other NMR experimental data. In particular, Phe[10], Leu[69], Val[81], Val[89], and Val[110] were identified from the selectively ^{15}N-enriched samples. Five residues have not yet been assigned (see Fig. 1). Three of these residues are in the N-terminal interdomain linker sequence, Pro[6], His[7], and Pro[8], and two residues in the SH2 domain, Trp[9] and Ser[88].

Assignments were completed using a combination of the ^{1}H-^{15}N HSQC, HCCH-TOCSY, ^{1}H-^{15}N TOCSY-HSQC, ^{1}H-^{15}N NOESY-HMQC, and the triple resonance experiments. The sequential resonance assignments for the backbone nuclei were primarily achieved using the 3D triple resonance experiments. The HNCA and HN(CO)-CA data were used to assign the $^{13}C^{\alpha}$ resonances and to correlate them with their sequential $^{13}C^{\alpha}(i-1)$ neighbors. In a similar manner, the HNCACB and CBCA(CO)NH data were used to obtain the $^{13}C^{\beta}$ resonances and their sequential $^{13}C^{\beta}(i-1)$ neighbors. Due to extensive overlap of $^{13}C^{\alpha}$ chemical shifts, the $^{13}C^{\beta}$ chemical shifts were essential in obtaining and confirming many of the sequential assignments. Figure 3 illustrates the use of both $^{13}C^{\alpha}$ and $^{13}C^{\beta}$ resonances in the sequential assignment procedure; connectivities for Leu[46] through Phe[50] are shown. The gradient-enhanced version of the HNCO experiment was used to assign the ^{13}CO resonances. The ^{15}N, H^{N}, $^{13}C^{\alpha}$, H^{α}, and ^{13}CO backbone chemical shift assignments for the Grb2 SH2 domain are listed in Table 2.

A combined analysis of the HCCH-TOCSY and ^{1}H-^{15}N HMQC-TOCSY data resulted in the complete or partial identification of the amino acid side-chain spin systems. The transfer of magnetization was often more efficient in the HCCH-TOCSY experiment. Partial side-chain assignments for H^{α} and sometimes H^{β} resonances were obtained from the ^{1}H-^{15}N HMQC-TOCSY data. An H^{α} resonance derived from the ^{1}H-^{15}N HMQC-TOCSY data was paired with its respective $^{13}C^{\alpha}$ resonance in the HCCH-TOCSY data to locate its side chain. Two additional proline side chains were identified in the HCCH-TOCSY data, but have not yet been assigned to Pro[6] or Pro[8]. Since His[7] and Trp[9] are unassigned, we cannot correlate NOEs from these residues to the proline H^{α} atoms and their side chains. Additional cross peaks are present in the 3D HCCH-TOCSY data set, which could belong to His[7], Trp[9], or Ser[88]. However, we cannot correlate them to an amide proton or ^{15}N in the 2D HSQC, 3D NOESY-HMQC, or 3D HMQC-TOCSY data sets. This may be due to rapid exchange of their amide protons with solvent, rendering them undetectable. The $^{13}C^{\beta}$ resonances and the ^{1}H partial side-chain assignments are listed in Table 3.

Secondary structure analysis

The empirical Chemical Shift Index (CSI) method, which is a public-domain program obtained from D.S. Wishart, has been used to predict the secondary structure of proteins without reference to NOE measurements (Wishart and Sykes, 1994). The CSI method relies upon the fact that certain types of chemical shifts fall within well-defined ranges, dependent upon their secondary structural environment. $^{1}H^{\alpha}$, $^{13}C^{\alpha}$, $^{13}C^{\beta}$ and ^{13}CO chemical shifts for a given residue are compared to a reference set of random coil values. For a given nucleus, the deviation from the random coil value in an upfield or downfield direction indicates whether the residue is part of an α-helix or a β-strand. Residues in a β-strand, for example, exhibit $^{13}C^{\alpha}$ and $^{13}C^{\beta}$ shifts that are upfield and downfield, respectively, of random coil values.

The overall consensus results determined from the CSI analysis of the four nuclei are summarized in Fig. 4. The input data in this analysis include the $^{1}H^{\alpha}$, $^{13}C^{\alpha}$, $^{13}C^{\beta}$ and ^{13}CO chemical shifts for each residue. In the figure, a stretch of four or more sequential residues with an index of −1 represents a region of α-helicity, and, similarly, a stretch with a +1 index indicates a β-strand region. Residues without bars in Fig. 4 represent loop regions. The individual chemical shift analyses from which the consensus diagram is composed are in good agreement (three or more of the four nuclei) for all of the secondary struc-

TABLE 2
BACKBONE CHEMICAL SHIFT ASSIGNMENTS (ppm) FOR THE Grb2 SH2 DOMAIN[a]

Residue	^{15}N	H^N	$^{13}C^\alpha$	H^α	^{13}CO	Residue	^{15}N	H^N	$^{13}C^\alpha$	H^α	^{13}CO
G1			45.05	4.01, 4.18	173.77	F57	121.14	9.87	56.16	4.82	175.33
I2[b]	118.38	8.22	61.02	4.19	176.41	K58	123.20	8.83	56.94	4.37	175.56
E3	123.40	8.69	56.32	4.30	176.31	V59	122.52	8.24	62.87	3.99	175.41
M4	120.41	8.45	55.03	4.46	175.57	L60	130.06	8.57	54.04	4.35	175.26
K5	121.75	8.19	54.12	4.52		R61	113.56	7.90	52.40	5.67	177.95
P6[c]						D62	119.78	8.05	51.53	5.04	178.79
H7[c]						G63	104.48	8.66	46.38	3.85, 3.95	174.78
P8[c]						A64	120.44	7.92	51.12	4.56	177.76
W9[c]						G65	105.60	8.11	45.07	3.60, 4.19	175.95
F10	121.86	8.09	57.85	5.34	175.32	K66	119.76	8.69	55.79	4.52	175.86
F11	125.51	8.66	57.66	4.43	175.33	Y67	116.15	8.98	56.73	5.56	176.97
G12	102.20	5.48	46.88	3.57, 3.80	174.57	F68	114.65	9.26	57.27	5.08	
K13	124.98	8.75	55.60	4.87	176.18	L69	115.07	9.36	55.75	4.65	177.67
I14	117.72	7.34	57.89	4.69		W70	117.33	8.88	57.86	5.16	174.55
P15			62.50	4.48	177.55	V71	117.28	8.48	64.70	3.84	175.27
R16	122.81	9.00	60.66	3.39	178.21	V72	121.42	8.40	63.66	3.48	174.41
A17	115.89	9.03	55.12	4.12	180.75	K73	120.30	7.70	54.31	4.74	176.34
K18	115.32	6.89	57.13	4.25	178.74	F74	115.62	9.25	56.55	4.89	176.32
A19	120.07	7.91	54.89	3.88	179.23	N75	116.45	9.50	54.68	4.85	175.41
E20	113.29	8.29	60.04	3.84	178.61	S76	107.68	7.62	56.59	4.63	173.98
E21	119.15	7.99	59.54	3.94	179.31	L77	118.73	8.66	56.62	3.55	178.14
M22	114.67	7.99	58.86	4.03	179.79	N78	112.88	8.38	56.83	4.24	176.88
L23	115.74	8.15	57.01	3.97	179.23	E79	115.49	7.59	58.98	3.98	178.11
S24	112.38	8.35	61.47	4.26	175.59	L80	120.68	6.81	58.40	2.15	
K25	115.32	6.91	55.70	4.31	177.70	V81	117.50	7.86	66.07	2.74	177.14
Q26	116.07	7.41	54.96	4.13	176.16	D82	113.74	7.71	57.50	4.14	180.32
R27	116.43	8.67	56.58	4.24	177.04	Y83	119.51	7.85	61.44	4.07	
H28	113.86	7.84	54.50	4.92	174.08	H84			58.03	5.22	174.08
D29	121.58	8.71	55.81	4.54	177.83	R85	114.47	7.37	58.06	4.61	178.45
G30	109.64	9.56	45.34	3.21, 5.03	174.79	S86	105.64	7.22	57.92	4.27	172.99
A31	122.86	7.58	53.10	5.03	177.73	T87	118.24	7.26	62.99	4.43	
F32	115.90	7.32	55.50	6.15	171.83	S88[c]				4.08	
L33	110.52	8.95	54.36	4.80	175.93	V89	118.21	8.32	62.45	3.60	173.46
I34	117.67	9.44	59.90	5.50	173.60	S90	108.77	7.66	54.33	4.62	174.72
R35	121.30	9.19	52.09	5.34	173.66	R91	122.49	8.57	56.89	3.90	176.63
E36	122.41	8.65	54.43	4.27	175.96	N92	112.95	8.14	53.43	4.74	174.24
S37	117.81	8.40	58.12	4.46	175.26	Q93	115.88	7.47	54.08	4.39	174.16
E38	122.75	9.03	58.25	4.03	177.07	Q94	119.76	8.67	54.85	3.99	173.03
S39	110.20	8.16	58.34	4.51	174.09	I95	122.53	7.97	60.41	3.85	172.92
A40	124.22	7.40	49.37	4.79		F96	124.16	8.49	54.60	4.89	176.35
P41			63.45	4.33	179.02	L97	117.23	8.21	55.28	4.41	
G42	111.34	9.95	45.05	3.30, 4.01	172.48	R98	120.22	8.26	54.28	4.65	174.08
D43	118.39	7.56	52.77	4.84	175.66	D99	118.96	8.65	55.34	4.74	178.27
F44	120.78	9.43	56.86	5.67	175.88	I100	118.99	8.94	62.98	3.83	176.03
S45	113.24	9.34	58.14	5.30	171.37	E101	123.81	8.93	55.26	4.57	176.63
L46	125.88	9.59	53.91	5.27	175.44	Q102	121.16	8.79	55.89	4.34	175.88
S47	123.02	9.29	58.60	5.65	172.66	V103	121.40	8.36	59.75	4.46	
V48	119.91	9.19	59.49	5.22	173.85	P104			63.08	4.38	
K49	126.95	9.20	56.39	4.54	175.65	Q105	118.81	8.49	55.55	4.26	
F50	127.37	8.79	58.85	4.65	175.18	Q106	118.37	8.12	53.17	4.38	
G51	118.43	9.34	46.48	3.53, 3.72	174.95	P107			63.08	4.42	
N52	121.83	8.89	53.01	4.78	174.32	T108	112.14	8.16	61.84	4.23	
D53	116.86	7.87	52.87	4.96	174.49	Y109	120.64	8.15	57.56	4.61	179.31
V54	118.31	8.36	61.39	4.49	175.02	V110	121.20	7.99	61.86	4.02	
Q55	123.23	8.88	54.08	4.28	174.13	Q111	123.60	8.38	55.66	4.26	177.76
H56	116.60	8.20	54.19	5.52	175.36	A112	130.64	8.06	53.69	4.13	

[a] Experimental conditions: 90% H_2O/10% D_2O, 5 mM sodium acetate, pH 5.3, 25 °C.
[b] Residue I2 is I53 in the full-length Grb2 protein.
[c] Unassigned residues.

tural elements except for one, β-strand βE. For this particular strand, the H^{α} values are the only chemical shifts that indicate an index for a β-strand.

The CSI results are confirmed for the α-helices, the central antiparallel β-sheet (β-strands B, C, D, D', E and F), and β-strand G by qualitative analysis of the ^{1}H-^{15}N NOESY-HMQC data. The expected H^{N}/H^{N} and H^{α}/H^{N} NOEs between β-strands in the central antiparallel β-sheet are designated with double-headed arrows in Fig. 5. The dashed lines in the figure denote hydrogen bonds, determined from hydrogen/deuterium exchange experiments (data not shown). Preliminary analysis of the NOE data shows that some of the β-strands are longer by one or two residues than indicated by the CSI results.

Comparison of secondary structure

A number of three-dimensional structures of SH2 domains have been determined and the structures of these proteins appear to be quite homologous. The secondary structural components of a typical SH2 domain consist of two α-helices (designated αA and αB) and eight β-strands (βA through βG), following the nomenclature of Eck et al. (1993). Of the eight strands, β-strands B, C, D, D', E and F comprise the central antiparallel β-sheet structure (as shown in Fig. 5). The crystal structure of the full-length Grb2 protein has recently been solved by Maignan et al. (1995). The coordinates for this structure are unavailable at this time, precluding a direct comparison of the secondary structural elements of the SH2 domain determined by crystallography versus the CSI method. Although little detailed structural information about the full-length Grb2 protein is known, the core structure of the SH2 domain, the central antiparallel β-sheet flanked by two α-helices, is similar to that predicted by the CSI method.

A sequence alignment and predicted secondary structure of 26 different SH2 domains has been proposed by Lee et al. (1994), based upon their crystal structure of the amino-terminal SH2 domain of Syp tyrosine phosphatase. Details of predicted secondary structural components for the SH2 domain of Grb2 from this sequence alignment will be compared with our results from the CSI method. A summary of the secondary structural elements determined from the CSI method as well as those predicted by the sequence alignment is given in Fig. 1.

In this NMR study, the six individual β-strands that typically form the central antiparallel β-sheet structure have been assigned for the Grb2 SH2 domain and are designated as follows: βB, extending from Ala^{31} through Glu^{36}; βC, from Gly^{42} through Lys^{49}; βD, from Asp^{53} through Phe^{57}; βD', from Leu^{60} through Asp^{62}; βE, from Tyr^{67} through Trp^{70}; and βF, from Val^{72} through Phe^{74}. βG exists as a short β-strand from Ile^{95} through Arg^{98}. All of the highly conserved residues in SH2 domains, including those residues involved in phosphotyrosine binding, are present in the expected secondary structural regions.

At this point in time, we cannot determine if residues Trp^{9} through Phe^{11} adopt a β-strand conformation (βA) or if these residues simply exist as part of the N-terminal loop. Since Trp^{9} and the three residues preceding it have not been assigned, we do not have their chemical shifts for input into the CSI program, nor are we able to check any NOE measurements involving these residues.

A comparison of the other β-strand regions of the Grb2 SH2 domain shows that they are in good agreement

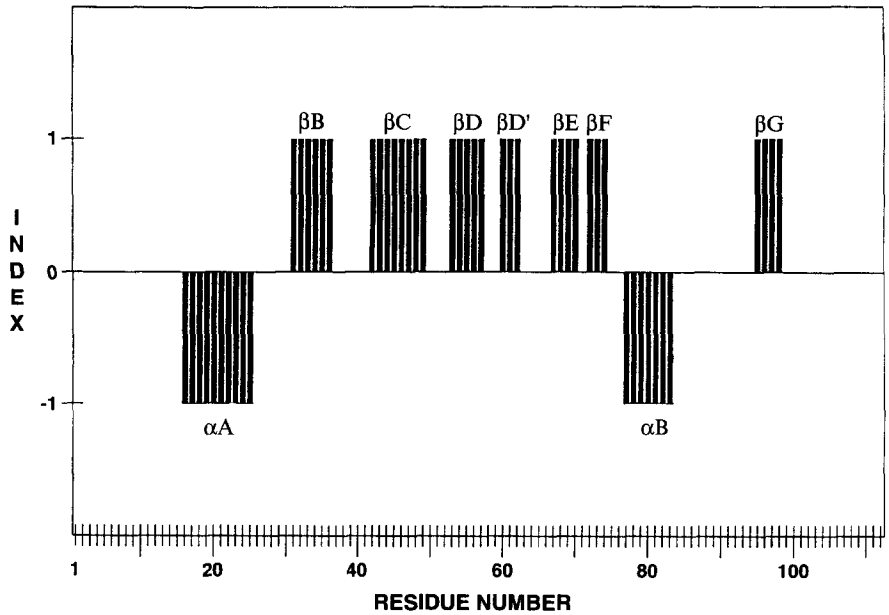

Fig. 4. CSI consensus diagram for the Grb2 SH2 domain, determined using four nuclei ($^{1}H^{\alpha}$, $^{13}C^{\alpha}$, $^{13}C^{\beta}$ and ^{13}CO). The secondary structural elements obtained from this program are summarized in the figure and below the amino acid sequence in Fig. 1.

TABLE 3
$^{13}C^{\beta}$ AND ^{1}H PARTIAL SIDE-CHAIN CHEMICAL SHIFT ASSIGNMENTS (ppm) FOR THE Grb2 SH2 DOMAIN[a]

Residue	$^{13}C^{\beta}$	$^{1}H^{\beta}$	$^{1}H^{\gamma}$	Others	Residue	$^{13}C^{\beta}$	$^{1}H^{\beta}$	$^{1}H^{\gamma}$	Others
G1					K58	32.89	1.74	1.41, 1.56	$C^{\delta}H_2$ 1.82;
I2[b]	38.88	1.86	1.20, 1.45	$C^{\gamma}H_3$ 0.92; $C^{\delta}H_3$ 0.87					$C^{\epsilon}H_2$ 2.99, 3.03
E3	30.05	1.95, 2.03	2.27		V59	30.57	2.30	0.79, 1.09	
M4	32.80	1.94	2.50		L60	41.55	0.09, 0.70	1.12, 1.46	
K5	32.56	1.65, 1.75	1.39, 1.44	$C^{\delta}H_2$ 1.44; $C^{\epsilon}H_2$ 2.96	R61	32.99	1.57, 1.78	1.34, 1.40	$C^{\delta}H_2$ 3.08
P6[c]					D62	42.40	2.50, 3.27		
H7[c]					G63				
P8[c]					A64	19.26	1.44		
W9[c]					G65				
F10	38.47	2.53, 2.79			K66	32.49	1.78, 1.98	1.44	$C^{\delta}H_2$ 1.49;
F11	40.70	2.56, 3.33							$C^{\epsilon}H_2$ 2.91, 2.97
G12					Y67	41.83	2.62, 2.77		
K13	31.13	1.67, 1.84	1.20	$C^{\delta}H_2$ 1.42, 1.74;	F68	41.80	2.72, 3.44		
				$C^{\epsilon}H_2$ 3.00	L69	44.20	1.05, 1.64	1.50	$C^{\delta}H_3$ 0.36, 0.75
I14	39.59	1.87	1.09, 1.55	$C^{\gamma}H_3$ 1.00; $C^{\delta}H_3$ 0.71	W70	29.76	3.43, 3.52		
P15	32.55	2.49	2.08		V71	33.97	1.83	0.54, 0.66	
R16	30.21	1.65	0.80, 1.20	$C^{\delta}H_2$ 2.77, 2.83;	V72	31.76	1.54	0.18, 0.88	
				$N^{\epsilon}H$ 7.14	K73	35.58	1.50, 1.73	1.10, 1.33	$C^{\delta}H_2$ 1.45,
A17	18.31	1.42							1.69; $C^{\epsilon}H_2$ 2.98
K18	31.50	1.92	1.52	$C^{\delta}H_2$ 1.75; $C^{\epsilon}H_2$ 2.99	F74	43.86	2.77, 3.44		
A19	18.21	1.42			N75	39.25	3.02		
E20	28.56	1.96, 2.14	2.39, 2.68		S76	66.84	3.51		
E21	29.79	2.19	2.12, 2.39		L77	40.80	1.12, 1.50	0.92	$C^{\delta}H_3$ 0.18, 0.35
M22	33.69	1.85, 2.04	2.34, 2.55		N78	38.20	2.74		
L23	42.39	1.15, 1.83	1.69	$C^{\delta}H_3$ 0.60, 0.70	E79	31.16	2.10, 2.32	2.36	
S24	63.00	3.91			L80	42.08	1.15, 1.68	1.44	$C^{\delta}H_3$ 0.54, 0.92
K25	32.87	1.76, 2.04	1.21, 1.53	$C^{\delta}H_2$ 1.44, 1.95;	V81	31.33	1.47	–0.27, 0.15	
				$C^{\epsilon}H_2$ 2.99	D82	39.79	2.57		
Q26	28.77	2.22	2.67		Y83	39.81	2.59, 2.99		
R27	30.85	1.50, 1.64	1.48	$C^{\delta}H_2$ 3.14; $N^{\epsilon}H$ 7.39	H84	27.06	2.61		
H28	30.92	2.64, 3.12		4H 7.08	R85	30.20	1.75		
D29	40.93	2.71, 2.83			S86	64.60	3.60, 3.85		
G30					T87	70.36	2.98	1.28	
A31	18.62	1.47			S88[c]				
F32	44.36	3.20			V89	31.90	1.42	0.30	
L33	45.65	1.73, 1.83	1.24	$C^{\delta}H_3$ 0.30, 0.75	S90	64.61	3.52		
I34	39.57	2.28	1.42, 1.89	$C^{\gamma}H_3$ 1.22; $C^{\delta}H_3$ 0.71	R91	30.09	1.34, 1.52	1.11	$C^{\delta}H_2$ 2.58
R35	33.88	1.34, 2.17	1.10, 1.49	$C^{\delta}H_2$ 2.57, 3.29;	N92	40.20	2.57, 2.71		
				$N^{\epsilon}H$ 6.69	Q93	33.03	1.44, 1.61	1.98, 2.16	
E36	32.78	1.91	2.19		Q94	28.29	1.61, 1.97	2.19	
S37	63.50	3.85, 4.17			I95	40.07	1.19	0.46, 0.56	$C^{\gamma}H_3$ –0.22;
E38	30.35	2.01, 2.10	2.18, 2.27						$C^{\delta}H_3$ 0.19
S39	64.17	3.74, 3.87			F96	40.43	2.64, 3.12		
A40	19.59	1.19			L97	39.63	0.56, 0.95	1.34	$C^{\delta}H_3$ –0.08,
P41	31.70	2.21	1.89	$C^{\delta}H_2$ 2.96					0.34
G42					R98	34.18	1.65, 1.84	1.73	$C^{\delta}H_2$ 3.21;
D43	41.70	2.69, 2.87							$N^{\epsilon}H$ 7.23
F44	41.69	2.88, 3.16			D99	40.79	2.60, 2.82		
S45	66.19	3.45, 3.66			I100	39.19	1.83	1.00, 1.67	$C^{\gamma}H_3$ 0.73;
L46	45.13	1.24, 1.97	1.64	$C^{\delta}H_3$ 0.59, 0.77					$C^{\delta}H_3$ 0.91
S47	65.72	3.42, 3.57			E101	31.98	2.07	2.31, 2.46	
V48	36.53	1.87	0.89		Q102	29.19	1.99, 2.07	2.34	
K49	34.76	2.12	1.39, 1.50	$C^{\delta}H_2$ 1.73; $C^{\epsilon}H_2$	V103	32.56	2.09	0.94, 1.01	
				2.96, 3.02	P104	32.16			
F50	40.77	2.84			Q105	29.61	2.01	2.38	
G51					Q106	30.02	1.85	2.05	
N52	38.64	2.69, 2.98			P107	32.09	1.74, 2.22	2.01	$C^{\delta}H_2$ 3.67, 3.81
D53	44.70	2.72			T108	69.75	4.13	1.17	
V54	33.74	1.78	0.44, 0.86		Y109	38.90	2.99		
Q55	31.68	1.41, 2.12	2.69, 2.84		V110	33.12	1.95	0.87	
H56	33.29	2.60, 2.77			Q111	29.61	1.95, 2.05	2.39	
F57	41.66	2.80, 3.05			A112	20.20	1.34		

[a] Experimental conditions: 90% H_2O/10% D_2O, 5 mM sodium acetate, pH 5.3, 25 °C.
[b] Residue I2 is I53 in the full-length Grb2 protein.
[c] Unassigned residues.

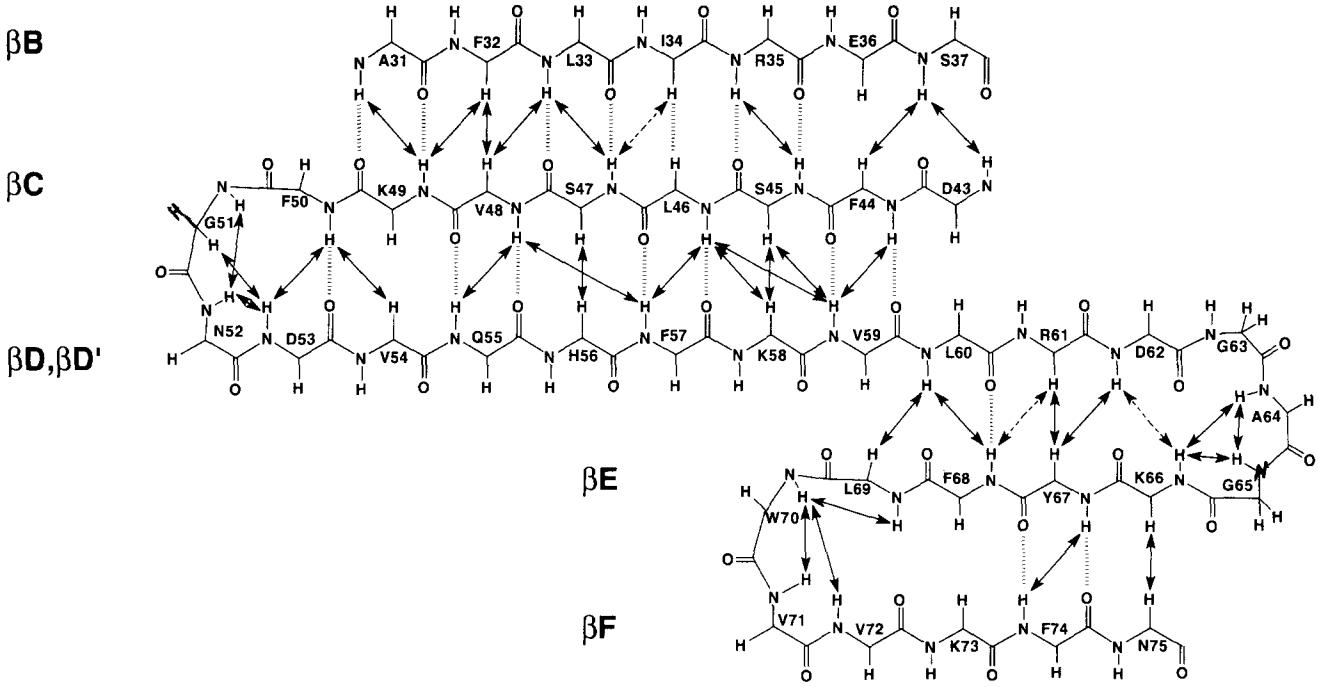

Fig. 5. Diagram of the central antiparallel β-sheet structure of the Grb2 SH2 domain with observed NOEs. Double-headed arrows designate an NOE between two nuclei. Dashed lines indicate hydrogen bonds determined from hydrogen/deuterium exchange experiments (data not shown). The β-strands are labeled according to the SH2 nomenclature previously established (Eck et al., 1993).

with the sequence alignment, except where the strands begin and end. For example, βB was predicted to extend from Ala[31] through Ser[37], whereas the CSI method shows that it ends one residue earlier, at Glu[36]. Another β-strand that is shifted slightly in sequence is βG, which is predicted by the sequence alignment to extend from Asp[99] through Glu[101]. The CSI method, however, indicates that this β-strand extends from Ile[95] through Arg[98].

The Grb2 SH2 domain also contains two α-helices: αA, extending from Arg[16] through Lys[25], and αB, extending from Leu[77] through Tyr[83]. The first α-helix, αA, is 10 residues long and begins and ends one residue later than is predicted by the sequence alignment. In contrast, the second α-helix, αB, is five residues shorter than the predicted α-helix. Discrepancies between the exact location of secondary structural elements for structures determined by X-ray methods and CSI consensus data have been noted for other proteins as well (Wishart and Sykes, 1994). The CSI results also indicate that the Grb2 SH2 domain is flanked by two large loops at the N- and C-terminal ends of the protein, as shown in Fig. 1. These loops contain terminal SH2 residues, residues that link the SH2 domain to the SH3 domains, as well as one or two residues from the SH3 domains.

Conclusions

Heteronuclear NMR data and the CSI method have been used to demonstrate that the secondary structure of a protein can be rapidly evaluated for comparison to homologous proteins, without analyzing all of the NOE data. In this NMR study, the secondary structure determined from the CSI results has been compared to that predicted for the Grb2 SH2 domain from a sequence alignment (Lee et al., 1994). In general, the location, character, and lengths of the secondary structural elements were found to be in good agreement between the two methods, with slight differences appearing at α-helix and β-strand termini. The largest differences were observed for helix αB and strand βG. The CSI results also agree with the core structure of the SH2 domain as determined by X-ray crystallography in the full-length Grb2 protein (Maignan et al., 1995).

Acknowledgements

The authors would like to extend special thanks to Dr. D.S. Wishart for the use of his CSI program and Ms. M. Berlyn at the *E. coli* Genetic Stock Center for the DL39 strain. We also thank Mr. V. Khadse for the N-terminal amino acid sequencing and the amino acid analysis, and Dr. E. Huang for the mass spectrometry analysis. We wish to extend special thanks to Dr. L.E. Kay for providing us with his gradient-enhanced pulse programs and to Dr. M. Summers for providing the Omega 3D TOCSY-HMQC pulse program. The authors wish to acknowledge Prof. J. Prestegard for helpful scientific input and for reading this manuscript. We thank Drs. T.M. Chan, C.A. Evans, P.W. Mui, and M.E. Snow for helpful discussions as well as for critical reading of this manuscript.

References

Bax, A., Clore, G.M. and Gronenborn, A.M. (1990) *J. Magn. Reson.*, **88**, 425–431.

Bax, A. and Ikura, M. (1991) *J. Biomol. NMR*, **1**, 99–104.

Bodenhausen, G. and Ruben, D.J. (1980) *Chem. Phys. Lett.*, **69**, 185–189.

Booker, G.W., Breeze, A.L., Downing, A.K., Panayotou, G., Gout, I., Waterfield, M.D. and Campbell, I.D. (1992) *Nature*, **358**, 684–687.

Brown, S.C., Weber, P.L. and Mueller, L. (1988) *J. Magn. Reson.*, **77**, 166–169.

Chardin, P., Camonis, J.H., Gale, N.W., Van Aelst, L., Schlessinger, J., Wigler, M.H. and Bar-Sagi, D. (1993) *Science*, **260**, 1338–1343.

Clark, S.G., Stern, M.J. and Horvitz, H.R. (1992) *Nature*, **356**, 340–344.

DeLoskey, R.J., Van Dyk, D.E., Van Aken, T.E. and Campbell-Burk, S. (1994) *Arch. Biochem. Biophys.*, **311**, 72–78.

Downward, J. (1994) *FEBS Lett.*, **338**, 113–117.

Eck, M.J., Shoelson, S.E. and Harrison, S.C. (1993) *Nature*, **362**, 87–91.

Farmer II, B.T., Venters, R.A., Spicer, L.D., Wittekind, M.G. and Mueller, L. (1992) *J. Biomol. NMR*, **2**, 195–202.

Griesinger, C., Otting, G., Wüthrich, K. and Ernst, R.R. (1988) *J. Am. Chem. Soc.*, **110**, 7870–7872.

Grzesiek, S. and Bax, A. (1992) *J. Am. Chem. Soc.*, **114**, 6291–6293.

Hatada, M.H., Lu, X., Laird, E.R., Green, J., Morgenstern, J.P., Lou, M., Marr, C.S., Philips, T.B., Ram, M.K., Theriault, K., Zoller, M.J. and Karas, J.L. (1995) *Nature*, **377**, 32–38.

Hensmann, M., Booker, G.W., Panayotou, G., Boyd, J., Linacre, J., Waterfield, M. and Campbell, I.D. (1994) *Protein Sci.*, **3**, 1020–1030.

Kay, L.E., Ikura, M., Tschudin, R. and Bax, A. (1990) *J. Magn. Reson.*, **89**, 496–514.

Kay, L.E., Xu, G.Y., Singer, A.U., Muhandiram, D.R. and Forman-Kay, J.D. (1993) *J. Magn. Reson. Ser. B*, **101**, 333–337.

Lee, C.H., Kominos, D., Jacques, S., Margolis, B., Schlessinger, J., Shoelson, S.E. and Kuriyan, J. (1994) *Structure*, **2**, 423–438.

LeMaster, D.M. and Richards, F.M. (1988) *Biochemistry*, **27**, 142–150.

Levy, G.C. and Lichter, R.L. (Eds) (1979) *Nitrogen-15 Nuclear Magnetic Resonance Spectroscopy*, Wiley, New York, NY.

Lowenstein, E.J., Daly, R.J., Batzer, A.G., Li, W., Margolis, B., Lammers, R., Ullrich, A., Skolnik, E.Y., Bar-Sagi, D. and Schlessinger, J. (1992) *Cell*, **70**, 431–442.

Maignan, S., Guilloteau, J.P., Fromage, N., Arnoux, B., Becquart, J. and Ducruix, A. (1995) *Science*, **268**, 291–293.

Marion, D. and Wüthrich, K. (1983) *Biochem. Biophys. Res. Commun.*, **113**, 967–974.

Marion, D., Ikura, M., Tschudin, R. and Bax, A. (1989a) *J. Magn. Reson.*, **85**, 393–399.

Marion, D., Driscoll, P.C., Kay, L.E., Wingfield, P.T., Bax, A., Gronenborn, A.M. and Clore, G.M. (1989b) *Biochemistry*, **28**, 6150–6156.

McIntosh, L.P. and Dahlquist, F.W. (1990) *Q. Rev. Biophys.*, **23**, 1–38.

Muchmore, D.C., McIntosh, L.P., Russell, C.B., Anderson, D.E. and Dahlquist, F.W. (1989) *Methods Enzymol.*, **177**, 44–73.

Muhandiram, D.R. and Kay, L.E. (1994) *J. Magn. Reson. Ser. B*, **103**, 203–216.

Narula, S.S., Yuan, R.W., Adams, S.E., Green, O.M., Green, J., Philips, T.B., Zydowsky, L.D., Botfield, M.C., Hatada, M., Laird, E.R., Zoller, M.J., Karas, J.L. and Dalgarno, D.C. (1995) *Structure*, **3**, 1061–1073.

Olivier, J.P., Raabe, T., Henkemeyer, M., Dickson, B., Mbamalu, G., Margolis, B., Schlessinger, J., Hafen, E. and Pawson, T. (1993) *Cell*, **73**, 179–191.

Overduin, M., Mayer, B., Rios, C.B., Baltimore, D. and Cowburn, D. (1992a) *Proc. Natl. Acad. Sci. USA*, **89**, 11673–11677.

Overduin, M., Rios, C.B., Mayer, B.J., Baltimore, D. and Cowburn, D. (1992b) *Cell*, **70**, 697–704.

Pascal, S.M., Singer, A.U., Gish, G., Yamazaki, T., Shoelson, S.E., Pawson, T., Kay, L.E. and Forman-Kay, J.D. (1994) *Cell*, **77**, 461–472.

Pawson, T. (1995) *Nature*, **373**, 573–580.

Shaka, A.J., Keeler, J. and Freeman, R. (1983) *J. Magn. Reson.*, **53**, 313–340.

Shaka, A.J., Barker, P.B. and Freeman, R. (1985) *J. Magn. Reson.*, **64**, 547–552.

Shaka, A.J., Lee, C.J. and Pines, A. (1988) *J. Magn. Reson.*, **77**, 274–293.

Songyang, Z., Shoelson, S.E., McGlade, J., Olivier, P., Pawson, T., Bustelo, X.R., Barbacid, M., Sabe, H., Hanafusa, H., Yi, T., Ren, R., Baltimore, D., Ratnofsky, S., Feldman, R.A. and Cantley, L.C. (1994) *Mol. Cell. Biol.*, **14**, 2777–2785.

States, D.J., Haberkorn, R.A. and Ruben, D.J. (1982) *J. Magn. Reson.*, **48**, 286–292.

Waksman, G., Kominos, D., Robertson, S.C., Pant, N., Baltimore, G., Birge, R.B., Cowburn, D., Hanafusa, H., Mayer, B.J., Overduin, M., Resh, M.D., Rios, C.B., Silverman, L. and Kuriyan, J. (1992) *Nature*, **358**, 646–653.

Waksman, G., Shoelson, S.E., Pant, N., Cowburn, D. and Kuriyan, J. (1993) *Cell*, **72**, 779–790.

Wishart, D.S. and Sykes, B.D. (1994) *J. Biomol. NMR*, **4**, 171–180.

Wittekind, M. and Mueller, L. (1993) *J. Magn. Reson. Ser. B*, **101**, 201–205.

Xu, R.X., Word, J.M., Davis, D.G., Rink, M.J., Willard, D.H. and Gampe Jr., R.T. (1995) *Biochemistry*, **34**, 2107–2121.

Zhou, M.M., Meadows, R.P., Logan, T.M., Yoon, H.S., Wade, W.S., Ravichandran, K.S., Burakoff, S.J. and Fesik, S.W. (1995) *Proc. Natl. Acad. Sci. USA*, **92**, 7784–7788.